

Structural Study of an Amorphous Bi-Fe-Ca-O Thin Film by the Anomalous X-ray Scattering

著者	Matsubara E., Waseda Y., Mitera M., Masumoto T.
journal or publication title	Science reports of the Research Institutes, Tohoku University. Ser. A, Physics, chemistry and metallurgy
volume	34
number	2
page range	155-170
year	1989-03-20
URL	http://hdl.handle.net/10097/28313

**Structural Study of an Amorphous Bi-Fe-Ca-O Thin Film
by the Anomalous X-ray Scattering***

E.Matsubara and Y.Waseda

Research Institute of Mineral Dressing and Metallurgy (SENKEN)

M.Mitera** and T.Masumoto

Institute for Materials Research

(Received September 19, 1988)

Synopsis

The structure of the amorphous Bi-Fe-Ca-O film with 0.3 μ m thick grown on the Si single crystal was studied by the anomalous x-ray scattering (AXS) method. This relatively new method using the anomalous dispersion effect of a specific constituent element in a film reduces the difficulty in the subtraction process of a substrate intensity for estimating the net intensity of a thin film, which becomes a main cause of errors of the resultant data in the conventional method. The environmental radial distribution functions around Bi and Fe in the amorphous Bi-Fe-Ca-O film were determined, from which the structural features were obtained.

I. Introduction

More information about physical and chemical properties of thin films is required for further developments of many kinds of films as new functional materials.¹ The X-ray diffraction is one of the methods which is frequently employed for the structural studies of the films. If a film is formed on a substrate which is relatively thin or consists of materials with low atomic numbers, or if the film can be removed from a substrate, the transmission method can be applied.² However, practically a substrate is always neither made of light elements nor removable from a film and then films are retained on a

* The 586th report of the Research Institute of Mineral Dressing and Metallurgy (SENKEN)

** Permanent Address: Laboratory of Amorphous Magnetic Devices, Sendai 980.

substrate in many cases. In this case, the reflection method with the Seemann-Bohlin arrangement with a small angle of incidence is employed. This method is widely used in the structural study of crystalline thin films, but very few applications have been actually made for non-crystalline films. This is mainly due to the difficulty in the subtraction process of a substrate intensity for estimating the net intensity of a thin film. The anomalous x-ray scattering (hereafter referred to as AXS) method recently appears to show reducing such difficulty.³

The main purpose of this paper is to present the fundamentals of this relatively new method using the anomalous dispersion effect for determining the atomic structure of an amorphous thin film grown on a substrate and to demonstrate its application to an amorphous Bi-Fe-Ca-O thin film of $0.3 \mu\text{m}$ thickness deposited on a silicon single crystal wafer of the (100) plane. This ferrite sample itself is also being drawn attention because the antiferromagnetic crystal of BiFeO_3 is recently found to convert into a ferromagnetic glass by adding CaO .⁴

II. Some Requirements for the Structural Analysis of Thin Films by X-rays

Figure 1 indicates a schematic diagram for the experimental set-up and its diffraction geometry of the Seemann-Bohlin arrangement⁵ employed in this work. Since a sample is irradiated with a small angle of incidence α , the penetration depth of x-rays becomes small and scattering from a surface is amplified relative to scattering from a bulk. The scattering intensity from the sample using this Seemann-

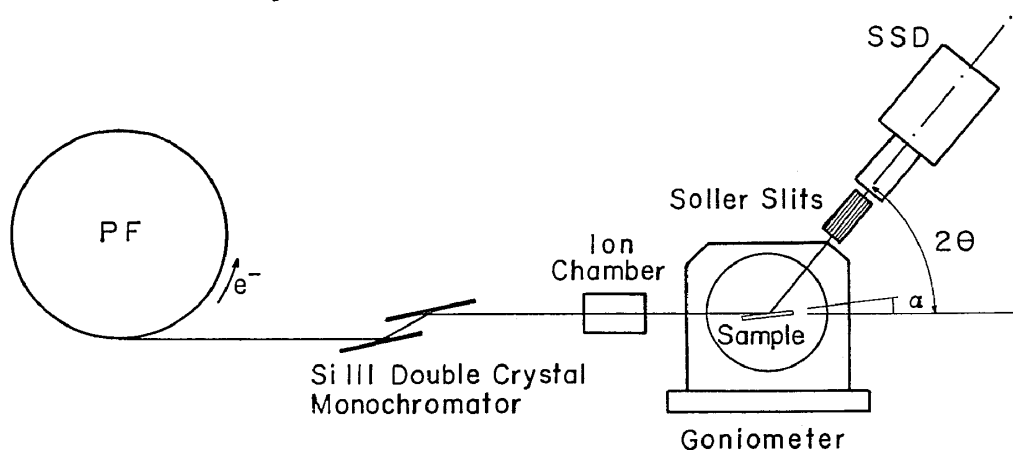


Fig. 1 Schematic diagram of experimental apparatus used for thin film measurements at the Photon Factory, Tsukuba.

Bohlin arrangement consists of the intensities from a thin film and a substrate holding it. Thus, in the quantitative structural analysis of a thin film grown on a substrate, the scattering intensity from the substrate should be subtracted from the total measured scattering intensity (I_t). The intensity of the substrate is usually estimated by applying the absorption correction (A_o) by the film to the intensity (I_s) measured in the same material as the substrate with the identical experimental condition. Namely, the intensity from a film alone (I_f) is expressed by:

$$I_f = I_t - A_o I_s, \quad (1)$$

and

$$A_o = \exp\left[-2\mu_f t_f \frac{\sin\theta \cos(\theta - \alpha)}{\sin\alpha \sin(2\theta - \alpha)}\right] I_s, \quad (2)$$

where μ_f and t_f are the linear absorption coefficient and thickness of the film, respectively.

The relation between the diffraction vectors and a section of the reciprocal lattice of the Si (100) substrate is schematically illustrated in Fig. 2. Since only the counter is scanned in the present case, the trace of the reflection vector \mathbf{S} becomes an arc and the counter is likely detect the tails of some Bragg reflections, such as (111) and (422) in this example. Therefore, the intensity profile appears to be very sensitive to the orientation of the sample placed on the holder. Because of this directional sensitivity of the

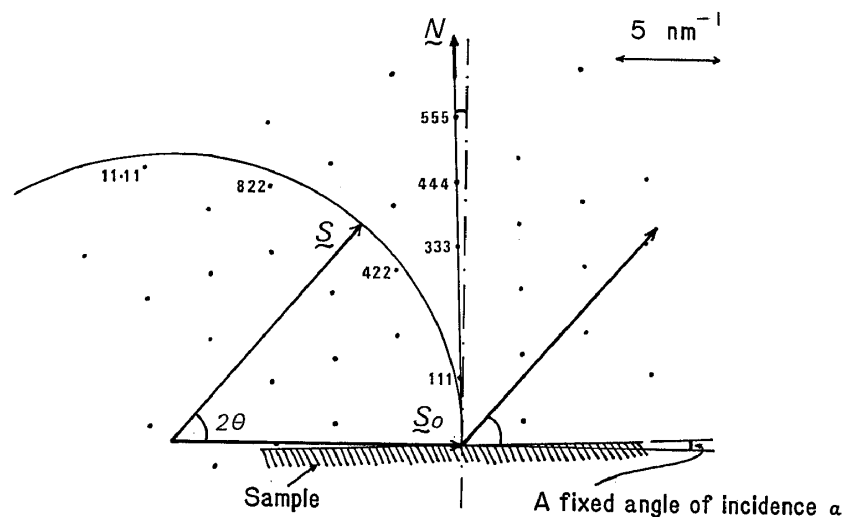


Fig. 2 Schematic diagram for the geometrical relation between the diffraction vectors and a section of the reciprocal lattice of the Si single crystal substrate.

scattering intensity, the orientational relation between two measurements of film plus substrate and substrate alone must be exactly identical. However, it is extremely difficult to carry out both the measurements of I_t and I_s under the exact experimental conditions especially when a single crystal is used as the substrate and the sample is detached from the holder in each measurement. In addition, the constants in the absorption correction term A_0 in eq.(2) must be determined precisely. These factors frequently produce some errors in the analysis of a thin film materials. It is easily imagined that these errors become more serious in a thinner film of sub-micron thickness. This is a reason why the application of the x-ray diffraction technique to the structural analysis of a thin film grown on a substrate is still limited. Thus, it is desirable to develop a new method which does not include the subtraction process in eq.(1) for a more precise and successful analysis even in a thinner film. With respect to this point, the use of AXS may result in a significant breakthrough in the quantitative structural analysis of a thin film, although the available data is still limited to only the preliminary data of an amorphous Ge film on a Si (111) wafer³.

III. Principle of the New Procedure using the AXS method

The radial distribution function (RDF) is widely used for the structural analysis of non-crystalline materials. However, most of non-crystalline materials of the present interest contain more than two kinds of atoms. Therefore, the local chemical environments around a specific element are required to describe the structure of multi-component systems, as well as the ordinary RDF data.

In order to determine the RDF in a non-crystalline system, the measured intensity must be converted into absolute units using the so-called normalization procedure such as the generalized Krogh-Moe-Norman method⁶ and the high angle method⁷. These normalization methods are also effectively applied to the analysis of a film grown on a substrate by subtracting the contribution of the substrate from the total intensity and obtaining the scattering intensity of the film alone, i.e. I_f in eq.(1)³. However, the new method using the AXS does not include this subtraction process. Therefore, a new conversion procedure to the absolute intensity is also introduced in this work. The fundamentals of this new method using the anomalous dispersion effect with a synchrotron radiation are given below.

As shown in Fig.1, the intensity of the incident beam is monitored by an ion chamber located in front of the sample during the measurements. The intensity of the ion chamber (I_m) is related with the power of the incident beam for a certain period of time (tP_0), that is,⁸

$$tP_0 = E_p I_m \exp(-\mu_i \frac{l_t + l_e}{2}) \exp(-\mu_a l_1) / (1 - \exp(-\mu_i l_e)) / E_i / e / G_a / G_v. \quad (3)$$

where t is the counting time which is the total monitor counts in the present study in order to compensate a gradual decrease in the incident beam intensity during the measurements with the synchrotron radiation. this study because of the reason explained below, E_p is the energy to form an ion-electron pair, μ_i and μ_a are the linear absorption coefficients of gas used for the ion chamber and air, respectively. l_t is the total length of the ion chamber and l_e the length of the electrode in the ion chamber, l_1 the distance from the ion chamber to the sample, E_i the energy of photons of incidence, e the electron charge, G_a the gain of the current amplifier and G_v the conversion gain of the voltage-frequency converter. By using eq.(3) for tP_0 , the intensity observed in the sample is given by:⁹

$$I_{obs}(Q, E) = C P \left(\frac{\rho_f A_f}{M_f} I_{eu,f}(Q, E) + \frac{\rho_s A_s}{M_s} I_{eu,s}(Q, E) \right), \quad (4)$$

where

$$A_f = \frac{\sin(2\theta - \alpha)}{2\mu_f \sin\theta \cos(\theta - \alpha)} \left[1 - \exp\left(-\frac{2\mu_f t_f \sin\theta \cos(\theta - \alpha)}{\sin\alpha \sin(2\theta - \alpha)}\right) \right], \quad (5)$$

$$A_s = \frac{\sin(2\theta - \alpha)}{2\mu_s \sin\theta \cos(\theta - \alpha)} \exp\left[-\frac{2\mu_f t_f \sin\theta \cos(\theta - \alpha)}{\sin\alpha \sin(2\theta - \alpha)}\right], \quad (6)$$

and

$$C = tP_0 (e^4/m^2/c^4) (wh/r^2) N_A. \quad (7)$$

The quantity of 2θ is the angle between the incident and diffracted beams, and μ_f and μ_s are the linear absorption coefficients of the film and substrate, respectively, $(e^4/m^2/c^4) = 7.9398 \times 10^{-30} \text{m}^2$, w and h are the width and height of the diffracted beam on the counter, r the distance from the sample to the counter, and N_A Avogadro's constant. The values of ρ_f and M_f are the density and atomic weight of the film respectively. ρ_s and M_s are similarly defined for the substrate.

$I_{eu,f}(Q,E)$ and $I_{eu,s}(Q,E)$ are the scattering intensities from the film and substrate in absolute units, respectively. P is the polarization term and almost equal to one for the synchrotron radiation.

The scattering factor of A in an n -component system can be expressed by:

$$f_A = f_A^0 + f'_A + if''_A, \quad (8)$$

where f_A^0 corresponds to the usual atomic scattering factor of A at an energy sufficiently away from the absorption edge of A , and f'_A and f''_A are the real and imaginary parts of the anomalous dispersion terms of A . As an example, the theoretical values of f' and f'' of Fe and Bi near their K and L_{III} absorption edges are shown in Fig. 3, respectively. It is confirmed^{10,11} that the values experimentally determined show a good agreement with the theoretical values^{10,12} at the lower energy side of the absorption edge but such an agreement is

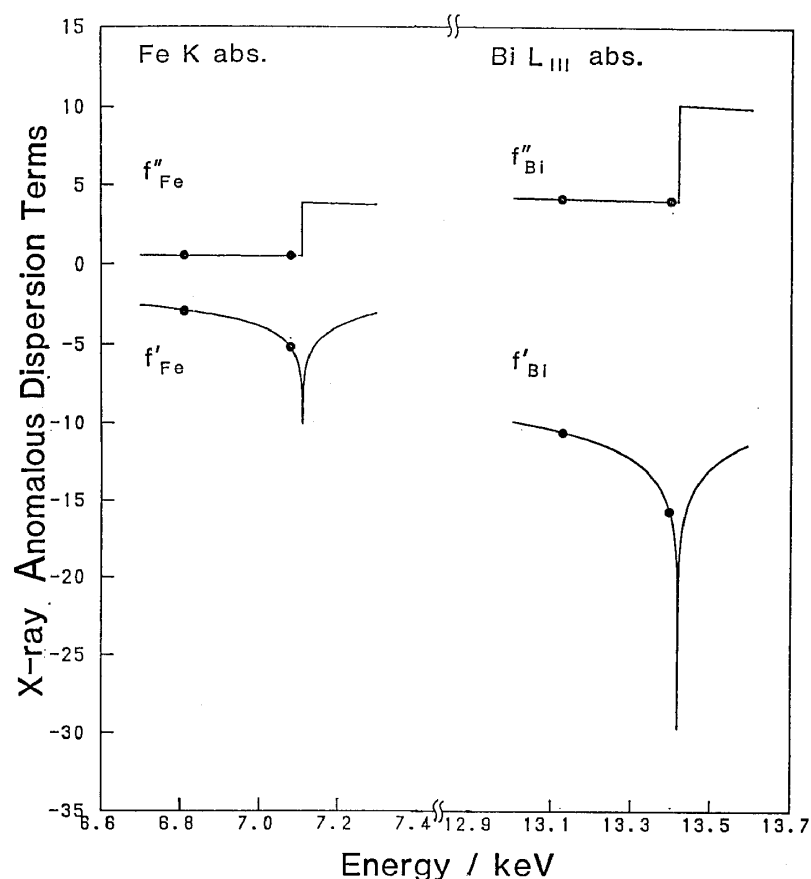


Fig. 3 Energy dependence of anomalous dispersion terms of Fe near the Fe K absorption edge and Bi near the L_{III} absorption edge. Solid curves correspond to the theoretical values computed by Cromer and Lieberman's method.¹² Solid circles indicate incident beam energies used in the present AXS measurement at each edge.

not detected at the higher energy side of the edge mainly due to the near edge structure and EXAFS.¹³ The values of f' show a drastic change at the lower energy side of the edge whereas f'' is small and almost constant at this energy region.

Let us consider that the energy of the incident beam is tuned near certain energy of the absorption edge of the element A. The atomic scattering factors of constituents other than the element A including the substrate (which is Si in the present case) are almost unchanged at this energy region because their absorption edges are usually far away from the absorption edge of A. The linear absorption coefficients of A are also almost equal in this energy region. Then, the following simplification can be made as shown in the previous work³.

The difference of the scattering intensities in absolute units measured at the two energies E_1 and E_2 below the absorption edge can be reduced to the following equation, using eq. (4).

$$\begin{aligned} \Delta I_{eu}(Q) &= I_{eu,f}(Q, E_1) - I_{eu,f}(Q, E_2) \\ &= \frac{1}{C P A_f} [I_{obs}(Q, E_1) - I_{obs}(Q, E_2)], \end{aligned} \quad (9)$$

By subtracting the difference of the mean square of the atomic scattering factors $\langle f^2 \rangle$ at these two energies from the intensity difference in eq. (9), the resultant intensity function ΔI is given as follows:

$$\begin{aligned} \Delta I &= \Delta I_{eu}(Q) - (\langle f^2(Q, E_1) \rangle - \langle f^2(Q, E_2) \rangle) \\ &= x_A (f'_A(E_1) - f'_A(E_2)) \sum_{j=1}^n \text{Re}[f_j(Q, E_1) + f_j(Q, E_2)] \\ &\quad \times \int_0^{\infty} 4\pi r^2 (\rho_{Aj}(r) - \rho_{Oj}) \frac{\sin Qr}{Qr} dr, \end{aligned} \quad (10)$$

where x_j is the atomic fraction of j element. It is easily understood from eq.(10) that, since the scattering from the substrate and Compton scattering from the sample are eliminated by taking the difference ΔI at the two energies E_1 and E_2 , the intensity ΔI enables us to provide the structural information of a film. In addition, the Fourier transform of ΔI defined by eq.(10) gives the environmental RDF around the element A in a film sample, that is,

$$4\pi r^2 \rho_{O+} + \frac{2r}{x_1 (f'_1(Q, E_1) - f'_2(Q, E_2))} \int_0^{\infty} \frac{Q \Delta I}{W(Q)} \sin Qr dQ$$

$$=4\pi r^2 \sum_{j=1}^n \frac{\text{Re}[f_j(Q, E_1) + f_j(Q, E_2)]}{W(Q)} \rho_{Aj}(r), \quad (11)$$

where

$$W(Q) = \sum_{j=1}^n x_j \text{Re}[f_j(Q, E_1) + f_j(Q, E_2)]. \quad (12)$$

Consequently, the environmental RDF around the atom A can be obtained without the difficulty in the subtraction process for the two measurements of the sample and the substrate plus sample when the AXS method is applied to the thin film analysis.

IV. Sample Preparation and Experimental Procedures

The sample preparation and the measurements of x-rays with the synchrotron radiation which are convenient for the present study are given below.

A mixture of 60 at%Fe₂O₃, 25 at%Bi₂O₃, and 15 at%CaO was sintered at a temperature above 1273 K. Then, it was melted at 1573 K, quenched in water, ground and thoroughly mixed. This process was repeated two times. The total time held at 1573 K through the preparation was 15 hrs. Then, the powder sample which was used as a target for sputtering was pelletized in a disk of 70 mm diameter and 2 mm thickness. A single crystal silicon wafer oriented along the [001] direction is cut into a rectangular shape of about 30 mm by 20 mm for a substrate material. The film of about 0.3 μm thickness was deposited by sputtering the target in Ar gas atmosphere at a sputtering pressure of 10 mTorr under a gas flow rate of 1.67×10⁻⁷ m³/s for 2 hrs. Only an upper half of the wafer was deposited and a lower half was left as the original Si (100) wafer. With this half-coated sample, the analysis by the conventional method including the subtraction process has also been carried out in order to obtain the average structure of the sample and to compare it with the environmental structure determined by the new AXS method. The sample was mounted on a goniometer head with the vertical translation³ so that the intensities from the sample (I_t) and from the substrate (I_s) were measured in an exactly identical diffraction geometry of the sample orientation and diffraction vector by simply changing the sample height.

The small angle of incidence α , which was precisely determined within 0.01° by aligning the sample with a parallel incident beam of a

0.05 mm wide, was set to 1° in the present measurement. The product of $\mu_f t_f$ was experimentally determined by taking a ratio of the integrated intensities of the Bragg peak of Si 400-reflection observed at the two different parts of the sample with and without coating. Since the film thickness was estimated to be 0.3 μm after preparation of the sample, the density was calculated 5.88 Mg/m^3 . This sample and its holder specially designed for the present measurement, and the careful determination of these constants α , μ_f and t_f , made it possible to obtain the profile of a film by the subtraction process. On the other hand, the sample position is fixed during the measurements by the new AXS method. Therefore, the sample or its holder specially prepared as above is not always required.

The measurement was carried out at a beam line (7C station) in the Photon Factory of the National Laboratory for High-Energy Physics, Tsukuba Japan. In this beam line, the monochromatic and horizontally polarized x-rays were obtained using a double Si 111 crystal monochromator from which any energy of incident beam from 4 to 20 keV was selected with the optimum energy resolution of about 7 eV at 10 keV. The incident beam was monitored by a N_2 gas ion chamber placed in front of the sample, and scattering intensity from the sample was measured at each angle for certain preset monitor counts in order to correct for the decay of the incident beam intensity during the measurements. At least 200,000 counts are collected at each scattering angle. Scattering intensities were measured with a Ge solid state detector so that the fluorescent radiation from the sample in the measurement near the absorption edge can be removed from the elastic scattering containing the structural information. The details of the experimental settings and the operating procedures are given in refs. 14 and 15.

V. Results and Discussion

First, the intensity measurement was carried out at the energy of 13.124 keV using the conventional method of the thin film analysis in order to obtain the ordinary RDF of the film for comparison. At this energy the effect of the anomalous dispersion terms on the total scattering is small. The intensity profiles of both the sample and absorption-corrected substrate are shown in **Fig.4**. The difference between them shown by a dotted line in the figure was corrected for the absorption by the film and converted to the absolute intensity

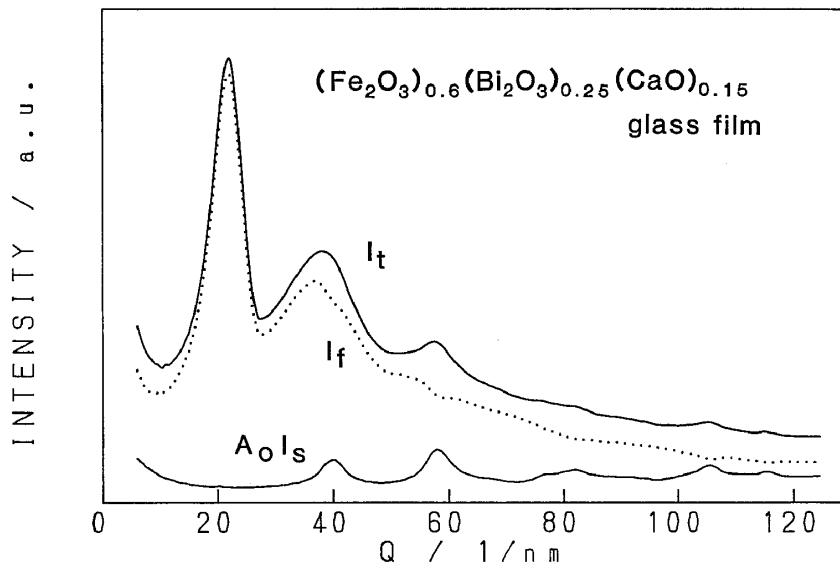


Fig. 4 X-ray scattering intensities of a $0.6Fe_2O_3-0.25Bi_2O_3-0.15CaO$ glass, I_t , and of a Si substrate corrected for the absorption by the glass film, $A_0 I_s$, and the difference between them, I_f at 13.124 keV.

with the generalized Krogh-Moe-Norman method, followed by the correction of the Compton scattering intensity theoretically estimated¹⁶. The total structural factor $S(Q)$ is estimated from this resultant intensity $I_{eu}(Q)$ in absolute units.

$$S(Q) = (I_{eu}(Q) - \langle f^2 \rangle + \langle f \rangle^2) / \langle f \rangle^2, \quad (13)$$

and

$$4\pi r^2 \rho(r) = 4\pi r^2 \rho_0 + \frac{2r}{\pi} \int_0^{\infty} Q[S(Q) - 1] \sin Qr \, dQ, \quad (14)$$

where $\langle f^2 \rangle - \langle f \rangle^2$ is the so-called Laue monotonic scattering. The Fourier transform of $S(Q)$ provides the ordinary RDF and $\rho(r)$ is the radial density function and ρ_0 is the average number density.

The incident beam energies of 6.811 and 7.086 keV, and of 13.124 and 13.399 keV indicated in solid circles in Fig. 3 were selected for the AXS measurements at the Fe K (7.111 keV) and Bi L_{III} (13.418 keV) absorption edges, respectively. Incidentally, these energies correspond to 300 and 25 eV below the respective edge. Although the energy of an incident beam is below the absorption edge, small fluorescent components were observed in the measurements near the edge, which mainly results from the tail of the band pass of the incident beam. In order to obtain a sufficiently reliable solution, such a fluorescent component should be eliminated from the total intensity¹⁰. The energy resolution of the Ge solid state detector is

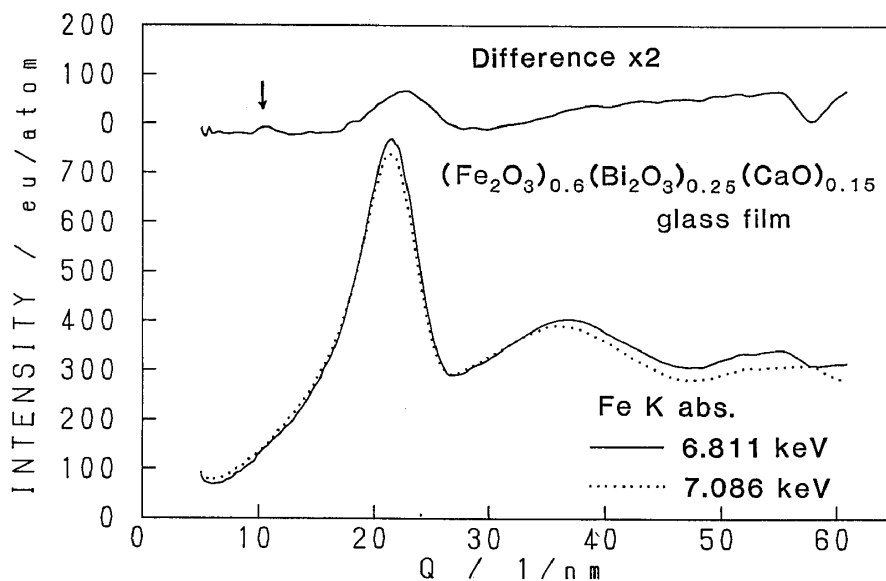


Fig. 5 Differential intensity profile of $0.6Fe_2O_3-0.25Bi_2O_3-0.15CaO$ glass (top) obtained from the intensity data (bottom) measured at incident energies of 6.811 and 7.086 keV which correspond to the energies of 300 and 25 eV below the Fe K absorption edge.

good enough to clearly separate the $K\alpha$ (6.401keV) or $L\alpha$ (10.831 keV) fluorescent radiation from the elastic scattering, but insufficient to separate the $K\beta$ (7.058 keV) or $L\beta$ (13.013 keV) fluorescence. However, since the intensity ratio $L\beta/L\alpha$ and $K\beta/K\alpha$ are known¹⁷, the intensity of the $L\beta$ or $K\beta$ component was estimated and subtracted in the data reduction process by monitoring the $L\alpha$ or $K\alpha$ component. After the correction of the absorption by air in a beam path, these intensities correspond to the intensity $I_{Obs}(Q,E)$ in eq. (4).

Two intensity profiles observed at the energies just below the Fe absorption edge are shown in Fig. 5. These intensities correspond to the intensities $I_{Obs}(Q,E_i)/CPA_f$ which appears in the right hand side of eq. (9). Thus, difference between these two intensities shown in the above of Fig. 5 corresponds to the intensity $\Delta I_{eu}(Q)$ defined in eq. (9). The maximum value of Q is somewhat limited for estimating the details of a local structure around Fe from the intensity profiles. However, the profile of the difference shows a small peculiar pre-peak near $10 nm^{-1}$. This pre-peak is hardly seen in the original profile since a large and long tail of the first peak extends to its low Q -side. In general, the presence of a pre-peak corresponds to compound-forming behavior.¹⁸⁻²⁰ Since the difference represents the atomic configurations around Fe, this pre-peak implies the presence of a chemical short-range ordering clusters around Fe in the alloys. Similarly, two intensity profiles observed at the energies just below the Bi L_{III} absorption edge and their difference are shown in Fig. 6.

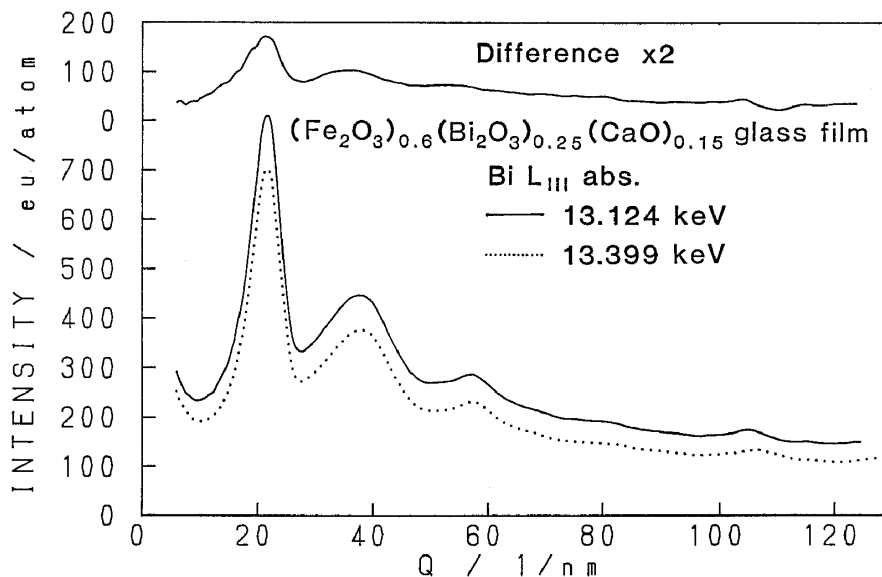


Fig. 6 Differential intensity profile of $0.6\text{Fe}_2\text{O}_3-0.25\text{Bi}_2\text{O}_3-0.15\text{CaO}$ glass (top) obtained from the intensity data (bottom) measured at incident energies of 13.124 and 13.399 keV which correspond to the energies of 300 and 25 eV below the Bi L_{III} absorption edge.

The intensity difference at the Bi L_{III} edge is much larger than the difference at the Fe K edge. This unexpectedly larger difference is explained by the much larger anomalous dispersion effect at the Bi L absorption edge. It is easily noted from the theoretical values drawn in Fig. 3 that the difference of the values of f' at the Bi L absorption edge appears to be about four times larger than the difference expected at the Fe K absorption edge. Consequently, it is found that the use of the L absorption edge is more efficient in this type of structural analyses by the anomalous dispersion effect.¹¹

The intensity difference ΔI in eq. (10) was computed from the difference $\Delta I_{\text{eu}}(Q)$ shown in Figs. 5 and 6 at each absorption edge. The Fourier transformation of ΔI in eq. (11) gives the environmental RDF around Fe or Bi. They are given in Fig. 7, together with the ordinary RDF calculated from the scattering measurements in Fig. 4. The profile in the environmental RDF around Fe is relatively broad since the upper limit of Q for Fourier transformation is much lower than the others, although such truncation effect is known not so significant when Q_{max} is larger than about 60 to 80 nm⁻¹. Before these RDFs are discussed, it is worth mentioning the following points. Since the sample of an amorphous Bi-Fe-Ca-O film contains four elements, the structure is essentially decomposed into ten possible atomic pairs, i.e. Bi-Bi, Bi-Fe, Bi-Ca, Bi-O, Fe-Fe, Fe-Ca, Fe-O, Ca-Ca, Ca-O, and O-O. However, the atomic pairs including Ca were ignored in the interpretation of the RDFs because the atomic fraction of Ca is much

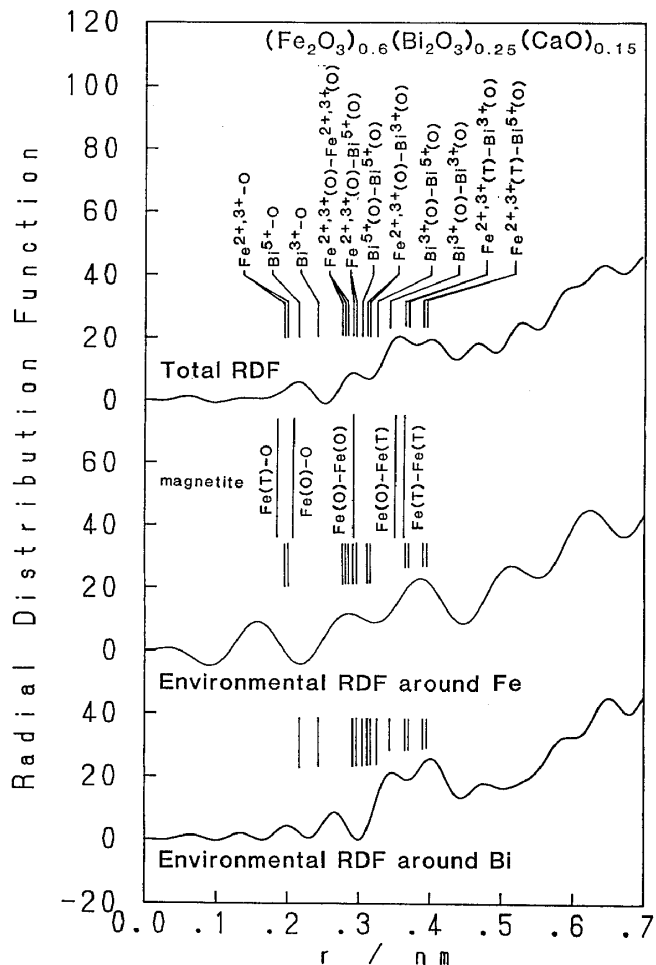


Fig. 7 Total radial distribution function (RDF) and environmental RDFs around Fe and Bi of a $0.6\text{Fe}_2\text{O}_3-0.25\text{Bi}_2\text{O}_3-0.15\text{CaO}$ glass.

less than the other three elements in the present system and the scattering factor of Ca is less than Fe and Bi. In spite of this assumption, the six partial structures still overlap in the ordinary RDF. But the environmental RDF around Fe contains mainly three partials of Fe-Fe, Fe-O, Fe-Bi, and similarly the environmental RDF around Bi consists of three partials of Bi-Bi, Bi-O, and Bi-Fe. As a result, by applying the AXS method, the relatively easier interpretation of the resultant RDFs is realized in the multi-component system. The following observation could be made from the results of Fig.7 with respect to the structural features of an amorphous thin film of the Bi-Fe-Ca-O system.

According to Mitera et al.⁴, the Fe atoms in this weak ferromagnetic glass is a mixture of Fe^{2+} and Fe^{3+} . By bearing these facts in mind, an atomic structure similar to the spinel structure was assumed as a model of the local atomic configurations in the

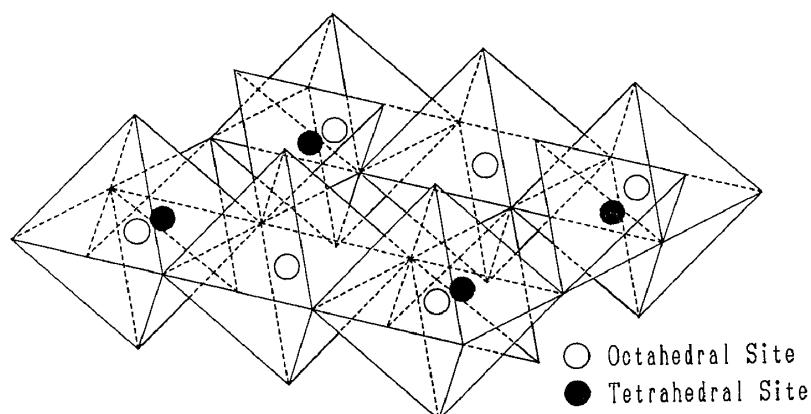


Fig. 8 Schematic diagram of a part of the configurations of the octahedral and tetrahedral sites in the spinel structure.

glass. A part of the spinel structure is schematically drawn in Fig. 8. As it is clearly seen in the figure, layers of cations located in the octahedral and tetrahedral sites formed by oxygen ions are orderly arranged in the spinel structure. Then, the distances between cations located in these two kinds of sites were estimated, referring ionic radii to Pauling's¹⁸, Ahrens'¹⁹ and Shannon-Prewitt's²⁰ values. The distances of cation- O^{2-} pairs were also estimated using these ionic radii. The distances of some possible pairs are indicated in Fig. 7 where capital letters "O" and "T" in the parentheses indicate the octahedral and tetrahedral sites, respectively. For comparison, some ion distances in the magnetite are also shown in the same figure. In the ordinary RDF, it seems that $(Fe^{2+}, Fe^{3+} \text{ or } Bi^{5+})-O^{2-}$ pairs are at the first peak and pairs of $(Fe^{2+} \text{ or } Fe^{3+})-(Fe^{2+} \text{ or } Fe^{3+})$, $(Fe^{2+} \text{ or } Fe^{3+})-Bi^{5+}$, or $Bi^{5+}-Bi^{5+}$ in the octahedral sites are possibly and mainly included at the second peak.

Only the positions of the possible ion pairs around Fe are indicated in the above of the curve of the environmental RDF around Fe. The first peak is located at a little lower value of r than the distance between $(Fe^{2+} \text{ or } Fe^{3+})$ and O^{2-} estimated from the ionic radii. The pairs of $(Fe^{2+} \text{ or } Fe^{3+})-(Fe^{2+} \text{ or } Fe^{3+})$, and $(Fe^{2+} \text{ or } Fe^{3+})-Bi^{5+}$ and $(Fe^{2+} \text{ or } Fe^{3+})-Bi^{3+}$ in the octahedral sites are located around the second peak of the environmental RDF around Fe. Similarly, the third peak is explained by the distance between Fe ions at the tetrahedral sites and Bi ions at the octahedral sites. Surprisingly, the distance estimated in the magnetite for the near-neighbor ion pairs in both sites appears to show a good agreement with the positions of the broad peak of the RDF curve although the RDF curve determined at Fe K edge includes some ambiguity in terms of the low

upper-limit in Q for the Fourier transformation. While it has been mentioned that the existence of the pre-peak in the profile of the intensity difference at the Fe K absorption edge indicates a strong chemical correlation between Fe and other ions. Since such a pre-peak is not observed in the profile of the intensity difference at the Bi L absorption edge in Fig. 6, the strong correlation between Fe ions causes the small pre-peak in the difference of the intensities measured near the Fe absorption edge.

The environmental RDF determined at the Bi L_{III} absorption edge represents the atomic configurations around Bi. For example, $(Bi^{3+}$ or $Bi^{5+})-O^{2-}$, $(Bi^{3+}$ or $Bi^{5+})-O-(Fe^{2+}$ or $Fe^{3+})$, or $(Bi^{3+}$ or $Bi^{5+})-O-(Bi^{3+}$ or $Bi^{5+})$ are possibly included. The first peak at 0.2 nm can be explained by $Bi^{5+}-O^{2-}$ pairs but not by $Bi^{3+}-O^{2-}$ pairs. The second peak at 0.27 nm seems not to be explained by any possible pairs. However, in a glass structure, it is not likely that the octahedral oxygen clusters do not orderly arranged in the same manner as in the crystal structure. Therefore, it is possible that the distance between cations in octahedral sites of the glass becomes closer than the distance in the crystal structure because of disordering of the octahedral clusters. From the above discussion, it is adequate that the second peak in the environmental RDF around Bi correspond to the distance between $(Fe^{2+}$ or $Fe^{3+})$ and Bi^{5+} ions in the octahedral sites. Consequently, it seems that Bi atoms become Bi^{5+} instead of Bi^{3+} in this system. Since Fe are a mixture of Fe^{2+} and Fe^{3+} according to Mitera et al.⁴, it is plausible that a charge transfer could happen in other cations.

The crystal $BiFeO_3$ has the perovskite structure, Fe atoms occupy only the octahedral site formed by six oxygens. However, such octahedron is not a favorable polyhedron for the glass formation, according to Zachariasen' rule.²¹ The present results rather indicate the coordination number of oxygen around Fe appears four. Thus, the ferromagnetic like behavior of an amorphous Bi-Fe-Ca-O system may be attributed to the formation of FeO_4 tetrahedra in this amorphous thin film. However, some further investigation is required for detailed discussion about the mechanism of magnetization in this oxide thin film.

Acknowledgments

A part of this research was supported by the Ishihara-Asada

Research Foundation and Iron and Steel Institute of Japan in 1987. We (EM and YW) particularly want to thank the staff of the Photon Factory, National Laboratory for High Energy Physics, Drs. T.Ishikawa and M.Nomura and Profs. T.Matsushita, H.Iwasaki and M.Ando.

Reference

- (1) see for example, J.D.Dow and I.K.Schuller (editors), *Interfaces, Superlattices and Thin Films*, MRS Symp. Proc., Vol.77 (1987).
- (2) W.E.Lukens and C.N.J.Wagner, *J. Appl. Cryst.*, **9**(1969),650.
- (3) E.Matsubara, Y.Waseda and H.Itozaki:*Trans.Japan.Inst.Metals*, **29**, (1988), 1.
- (4) M.Mitera, M.Mimura, S.Ohta and S.Masuda:Final Report of Sozo-Kagaku-Gijutsu-Suishin-Jigyo (Masumoto Project), (1986), p.7.
- (5) K.L.Weiner, *Zeit. fur Krist.*, **123**(1966),315.
- (6) C.N.J.Wagner, H.Ocken and M.L.Joshi:*Z.Naturforsch.*, **20a**, (1965), 325.
- (7) N.S.Gingrich:*Rev.Mod.Phys.*, **15** (1943), 90.
- (8) E.Matsubara and P.Georgopoulos:*J.Appl.Cryst.*, **18** (1985), 377.
- (9) L.H.Schwartz and J.B.Cohen:*Diffraction from Materials*, Academic Press, New York, 1977.
- (10) Y.Waseda:*Novel Application of Anomalous X-ray Scattering for Structural Characterization of Disordered Materials*, Springer-Verlag, Heiderberg, 1984.
- (11) E.Matsubara, Y.Waseda, M.Mitera and T.Masumoto:*Trans. Japan Inst. Metals*, **29**, (1988), 697.
- (12) D.T.Cromer and D.Lieberman:*J.Chem.Phys.*, **53** (1970), 1891.
- (13) B.K.Teo:*EXAFS Basic Principles and Data Analysis*, Springer-Verlag, Berlin Heidelberg, 1986.
- (14) Y.Waseda, E.Matsubara and K.Sugiyama:*Sci.Rep.Res.Inst.Tohoku Univ.*, **34A** (1987), 1.
- (15) M.Nomura, KEK Report Internal, No.87-1,(1987).
- (16) *International Tables for X-ray Crystallography*, Vol.IV, The Kynoch Press, Birmingham, 1974.
- (17) N.V.Rao, S.B.Reddy, G.Satyanarayana and D.L.Sastry:*Physica*, **138C**, (1986), 215.
- (18) L.Pauling, *The nature of the Chemical Bond*, Cornell Univ. Press, Ithaca, New York, (1945).
- (19) L.H.Ahrens, *Geochim Cosmochim. Acta*, **2**(1952),155.
- (20) R.D.Shannon and C.T.Prewitt:*Acta Crystallogr.*, **B25**, (1969), 925.
- (21) W.H.Zachariasen, *J. Amer. Chem.*, **54**(1932),3841.